

# Effects of the size and morphology of zinc oxide nanoparticles on the germination of Chinese cabbage seeds

Lei Xiang · Hai-Ming Zhao · Yan-Wen Li · Xian-Pei Huang ·  
Xiao-Lian Wu · Teng Zhai · Yue Yuan · Quan-Ying Cai · Ce-Hui Mo

Received: 31 October 2014 / Accepted: 22 January 2015 / Published online: 28 February 2015  
© Springer-Verlag Berlin Heidelberg 2015

**Abstract** The toxicity of four zinc oxide nanoparticles (i.e., spheric ZnO-30, spheric ZnO-50, columnar ZnO-90, and hexagon rod-like ZnO-150) to the seed germination of Chinese cabbage (*Brassica pekinensis* L.) was investigated in this study. The results showed that zinc oxide nanoparticles (nano-ZnOs) did not affect germination rates at concentrations of 1–80 mg/L but significantly inhibited the root and shoot elongation of Chinese cabbage seedlings, with the roots being more sensitive. The inhibition was evident mainly during seed incubation rather than the seed soaking process. Both the production of free hydroxyl groups (·OH) and the Zn bioaccumulation in roots or shoots resulted in toxicity of nano-ZnOs to Chinese cabbage seedlings. The toxicity of nano-ZnOs was affected significantly by their primary particle sizes in the minimum dimensionality, but large columnar ZnO-90 and small spherical ZnO-50 had comparable toxicities. Therefore, both the particle size and morphology affected the toxicity of nano-ZnOs.

**Keywords** Zinc oxide · Nanoparticles · Size · Morphology · Seed germination · Toxicity

## Introduction

Nanoparticles, with at least one dimension of 100 nm or less, fall in a transitional zone between individual molecules and the corresponding bulk materials (Lin and Xing 2007). Nanoparticles exhibit unique physical and chemical characteristics that differ from their bulk forms (Lin and Xing 2008). Due to their unique diverse nanostructures and excellent properties (e.g., photocatalysis, electrical conductivity, and chemical reactivity), engineering nanoparticles (ENPs) are applied in a diverse range of industries (e.g., electronics, optics, food packaging, textiles, medical devices, cosmetics, water treatment technology, fuel cells, catalysts, and biosensors) (Ghodake et al. 2011). In 2010, the number of nanotechnology products registered at the Woodrow Wilson International Center for Scholars was 1015, but only 475 in 2005 (Judy et al. 2011; Zhang and Karn 2005). The nanotechnology market is predicted to be worth \$1 trillion and to employ about two million workers by 2015 (Zhang et al. 2008).

Because of their increasing and large-scale production, usage, and disposal, ENPs can be released into the environment (Lin and Xing 2007, 2008; Rico et al. 2011). More than 95 % of ENPs that enter wastewater treatment plants are sequestered into sewage sludge and are thus removed from the effluent stream. ENPs may enter soil following the land application of sewage sludge (Kaegi et al. 2011). Using a model based on probabilistic material flow analysis, the concentrations of ENPs in sludge-treated soil in the USA were predicted to be 0.5 mg/kg for nano-TiO<sub>2</sub>, 22.3 µg/kg for nano-ZnO, 7.4 µg/kg for nano-Ag, and 0.4 µg/kg for carbon nanotubes (CNTs)

Responsible editor: Philippe Garrigues

**Electronic supplementary material** The online version of this article (doi:10.1007/s11356-015-4172-9) contains supplementary material, which is available to authorized users.

L. Xiang · H.-M. Zhao · Y.-W. Li · X.-P. Huang · X.-L. Wu ·  
T. Zhai · Y. Yuan · Q.-Y. Cai (✉) · C.-H. Mo (✉)

Key Laboratory of Water/Soil Toxic Pollutants Control and  
Bioremediation of Guangdong Higher Education Institutions,  
School of Environment, Jinan University, Guangzhou 510632,  
People's Republic of China  
e-mail: cai\_quanying@yahoo.com  
e-mail: tchmo@jnu.edu.cn

T. Zhai  
School of Chemistry and Chemical Engineering, Sun Yat-Sen  
University, Guangzhou 510275, People's Republic of China

(Gottschalk et al. 2009). Complex physicochemical and biochemical processes involving ENPs can occur in the plant-soil system and thus have unpredictable effects (Dietz and Herth 2011; Kool et al. 2011; Nair et al. 2010; Rousk et al. 2012). Plants can function as a pathway for the transportation of ENPs and as a route of bioaccumulation into the food chain, posing a threat to human health (Lin and Xing 2008; Ma et al. 2010; Zhu et al. 2008).

A few studies have reported the effects of nanoparticles on higher plants (Wang et al. 2012; Zhang et al. 2012). For example, Ma et al. (2010) reported that nano-CeO<sub>2</sub>, nano-La<sub>2</sub>O<sub>3</sub>, and nano-Gd<sub>2</sub>O<sub>3</sub> could significantly inhibit root elongation of seven higher plant species (radish, rape, tomato, lettuce, wheat, cabbage, and cucumber), but no inhibitions of root elongation in the six plants (except lettuce) were observed in nano-CeO<sub>2</sub> treatment. Lin and Xing (2007) reported that the root elongations of radish, rape, and ryegrass were inhibited significantly by nano-Zn and nano-ZnO. Nano-CuO significantly reduced growth of maize seedlings and was more readily absorbed, transported, and accumulated in the higher plants compared with micron CuO, due to its high surface-to-volume ratio and surface reactivity (Wang et al. 2012). Ryegrass root elongation was inhibited markedly under exposure to 50 mg/L nano-ZnOs (Lin and Xing 2008). Nanoparticulate Yb<sub>2</sub>O<sub>3</sub> had a greater effect on cucumber root length than bulk Yb<sub>2</sub>O<sub>3</sub> (Zhang et al. 2012). Nano-C<sub>70</sub>, nano-ZnO, and nano-Fe<sub>3</sub>O<sub>4</sub> could be taken up and accumulated by allium cepa, soybean, and pumpkin, respectively (Rico et al. 2011). However, the mechanism of the phytotoxicity of ENPs is unclear, with factors such as chemical composition, reactive oxygen species (ROS) derived from surface-catalyzed reactions, considered potential causes of ENP toxicity, especially for metal-based nanoparticles (Lin and Xing 2007; Yang and Watts 2005). A few studies have assessed the effects of ENP surface characteristics, size, and/or morphology on their nanotoxicity to higher plants (Yang and Watts 2005).

Zinc oxide nanoparticles (nano-ZnOs) are used increasingly in various products, such as coatings, personal care products, and chemical sensors or biosensors, due to their UV absorption and transparency to visible light (Luna-delRisco et al. 2011; Poynton et al. 2011). In recent years, ZnO nanoparticles with diverse morphologies (such as nanospheres, nanorods, and nanotubes) and sizes have been synthesized via various techniques (Zhai et al. 2012). However, the effects of the particle morphology and size of nano-ZnOs on the environment remain unclear. Seed germination and root/shoot elongation tests have been used to assess short-term phytotoxicity for evaluation of the ecological risks posed by emerging pollutants such as ENPs (Ma et al. 2010) and graphene (Hu and Zhou 2014). These bioassays have several advantages such as their suitability as a stand-by test method and their rapidity (Lin and Xing 2007; Ma et al. 2010).

Chinese cabbage (*Brassica pekinensis* L.) is an economically important and widely consumed vegetable in China and is often used in seed germination and root/shoot elongation toxicity tests (Liu et al. 2009a). In this study, Chinese cabbage was used for short-term phytotoxicity test of nano-ZnOs. The objectives of the present study were to investigate the effects of four nano-ZnOs with diverse size and morphology on the seed germination rates and seedling root/shoot growth of Chinese cabbage, and to evaluate the effects of particle size and morphology on the toxicity of nano-ZnOs to higher plants.

## Experimental section

### Materials

Four nano-ZnOs of diverse size and morphology were used: ZnO-30, ZnO-50, ZnO-90, and ZnO-150. The ZnO-30, ZnO-50, and ZnO-90 particles were purchased from WanJing Nanotech Co., Ltd. (Hangzhou, China), and ZnO-150 was provided by the School of Chemistry and Chemical Engineering, Sun Yat-Sen University (Guangzhou, China). Chinese cabbage seeds were purchased from the Vegetable Research Institute, Guangdong Academy of Agricultural Sciences (Guangzhou, China). The average germination rate of the seeds was greater than 90 % according to a preliminary test using deionized water (Supplementary data Fig. S1). Seeds were kept in a dry, dark place at room temperature until use. Deionized water was used for all seed germination tests. All other chemical reagents were of analytical grade. The Zn<sup>2+</sup> form used in tests was ZnSO<sub>4</sub>·7H<sub>2</sub>O, and 30 % H<sub>2</sub>O<sub>2</sub> was used for surface sterilization of the seeds. All reagents were purchased from Guangzhou Chemical Reagent Co., Ltd. (Guangzhou, China).

### Methods

#### *Nano-ZnO characterization*

The purity of the nano-ZnOs was determined using an atomic absorption spectrometer (AAS: AA7700, Shimadzu, Japan) at a wavelength of 213.9 nm. The size and morphology of the nano-ZnOs were investigated using transmission electron microscopy (TEM: JEM-2100 F, JEOL Ltd., Tokyo, Japan). For further evaluation of morphology, ZnO-150 was also subjected to scanning electron microscopy (SEM: JSM-6330 F, JEOL Ltd., Tokyo, Japan). The primary size distributions of these nano-ZnOs were determined from TEM images using ImageJ 2.1.4.7 (count of more than 100 particles for each nano-ZnO). The hydrodynamic diameters of the nano-ZnOs were measured by a dynamic light scattering method using a Zetasizer Nano ZS particle sizer (Malvern Instruments,

Malvern, UK). The surface areas of the nano-ZnOs were measured by a nitrogen adsorption/desorption method, with a physisorption analyzer (Micromeritics Tristar 3000, Norcross, GA, USA) at 77 K.

#### *Preparation of nano-ZnO suspensions and zinc ion ( $Zn^{2+}$ ) solution*

Stock suspensions of nano-ZnOs (1000 mg/L) were freshly prepared by adding nano-ZnOs to deionized water and dispersed by ultrasonic vibration (100 W, 40 kHz) (Ultrasonic instrument, KQ-250E, Kunshan, China) for 30 min. Suspensions of nano-ZnOs at concentrations 0, 1, 5, 10, 20, 40, and 80 mg/L were prepared by dilution of the stock suspensions with deionized water. The suspensions were stirred for 1 min using small magnetic bars before use to prevent the aggregation of nanoparticles. Zinc ion ( $Zn^{2+}$ ) solution was prepared by dissolving  $ZnSO_4 \cdot 7H_2O$  in deionized water.

#### *Seed germination*

Seed germination tests were conducted according to the Ecological Effects Test Guidelines-OPPTS 850.4200 (US EPA). Briefly, Chinese cabbage seeds were surface-sterilized in 3 %  $H_2O_2$  (v/v) for 10 min and then washed thoroughly with deionized water. Treated seeds were evenly placed onto Petri dishes (9 cm of inner diameter and 20 seeds per dish) with individual filter papers and the tested nano-ZnO suspensions/ $Zn^{2+}$  solutions. Petri dishes were covered with tape and placed in the dark in a constant-temperature incubator (PYX-250Q-A: KELI Co., Guangzhou, China) at 25 °C for germination. During germination, the seeds were exposed to 5-mL nano-ZnO solutions with concentrations at 1, 5, 10, 20, 40, and 80 mg/L. These concentrations were determined in a preliminary experiment, as they induced 10–60 % inhibition of root elongation. Seed germination in deionized water served as the control. Each treatment had three replicates. After 72 h of exposure, the germination rate, root length, and shoot length of the seedlings were measured. Zinc concentrations in the supernatants of nano-ZnOs suspensions before and after seed germination were measured by AAS (AA7700, Shimadzu) after centrifugation (3000g for 1 h) and filtration (0.22- $\mu$ m microporous membrane) following the method described by Lin and Xing (2007). pH values were also measured.

#### *Seed soaking assay*

Seed germination is normally considered to be a physiological process beginning with water imbibition by seeds (seed soaking process), and then the rootlet absorbing water after its emergence (incubation process) (Kordon 1992). To determine the process (seed soaking or incubation) being primarily responsible for the inhibition of root growth during seed

germination, three treatments were conducted, as described in previous studies (Lin and Xing 2007; Ma et al. 2010).

- Treatment I (ZnO- $H_2O$ ): Chinese cabbage seeds were soaked in a 40 mg/L nano-ZnO suspension for 2 h (during this period, seeds can thoroughly expose to nano-ZnO suspensions and not show the emergence of a radicle or cotyledon from the seed coats), rinsed for five times with deionized water, and then incubated in deionized water for 70 h.
- Treatment II ( $H_2O$ -ZnO): Seeds were soaked in deionized water for 2 h and then incubated in a 40 mg/L nano-ZnO suspension for 70 h.
- Treatment III (ZnO-ZnO): Seeds were soaked and incubated in a 40 mg/L nano-ZnO suspension for 72 h. All the four nano-ZnOs used in this study were evaluated by the three treatments above.

#### *Dimethyl sulfoxide (DMSO)-treated nano-ZnOs assay*

Three seed germination treatments, as described by a previous study (Yang and Watts 2005), were undertaken to determine the toxic effects of free hydroxyl groups ( $-OH$ ) derived from nano-ZnOs on root elongation of Chinese cabbage during seed germination.

- Treatment I (DMSO): Seeds were incubated in a solution with 1 % DMSO (v/v) for 72 h.
- Treatment II (ZnO): Seeds were placed in 40 mg/L nano-ZnO suspensions for 72 h.
- Treatment III (DMSO-ZnO): Seeds were germinated for 72 h in 40 mg/L nano-ZnO suspensions with 1 % DMSO (v/v), which was obtained by adding 2 mL of nano-ZnO stock suspension (100 mg/L) and 50  $\mu$ L of DMSO to 5 mL of deionized water.

#### *Determination of total zinc concentrations in roots and shoots*

To evaluate nano-ZnO uptake by Chinese cabbage seedlings, seeds were exposed to 1, 5, 10, 20, 40, and 80 mg/L nano-ZnO suspensions and 0, 0.5, 1, and 2 mg/L  $Zn^{2+}$  solution (in the form of  $ZnSO_4$ ), and the total zinc concentrations in roots and shoots were measured after seed germination. Seed germination experiments were conducted in triplicate for each concentration. The seedlings were then collected and washed thoroughly with both tap and deionized water orderly. Shoots and roots were separated, and their biomass was measured after drying at 50 °C for 12 h. Total Zn concentrations in the shoots and roots were determined by AAS after digestion in  $HNO_3$ .

Statistical analyses

Statistical analyses, including calculation of average values, standard deviation (SD), regression, and analysis of variance, were performed using SPSS 17.0. A one-way analysis of variance (ANOVA) followed by a Duncan’s (D) test or two-tailed Student’s *t* test was conducted to compare the significance of seed germination between control and nano-ZnO treatments and to compare the toxicity of the various nano-ZnO treatments. Subsequently, a two-way ANOVA was used to determine the effects of the sizes and concentrations of nano-ZnOs on their toxicity. Statistical significance was accepted at  $P < 0.05$ . The 50 % ( $IC_{50}$ ) and 10 % ( $IC_{10}$ ) inhibitory concentrations were calculated from regression equations.

Results

Particle characterization of nano-ZnOs

The purities of the four nano-ZnOs were greater than 99.5 %. The surface areas of ZnO-30, ZnO-50, ZnO-90, and ZnO-150 were 65, 55, 25, and 12 m<sup>2</sup>/g, respectively. SEM and TEM images of the four nano-ZnOs (Fig. 1) showed that ZnO-30 and ZnO-50 particles were spherical, and their average primary sizes were 30±12.5 and 50±20 nm (Supplementary data Fig. S2). ZnO-90 was columnar, and its average primary length and cross-sectional diameter were 400±300 and 90±

45 nm, respectively. ZnO-150 was hexagon rod-like, and its average length and hexagonal side length of ZnO-150 were 600±200 and 150±100 nm, respectively. All four nano-ZnOs aggregated upon dispersal in deionized water. The average hydrodynamic diameters of ZnO-30, ZnO-50, ZnO-90, and ZnO-150 were 562±103, 889±181, 1453±176, and 1920±249 nm, respectively (Supplementary data Fig. S3). Remarkably, the average hydrodynamic diameters of all four nano-ZnOs were positively correlated with their primary sizes in the minimum dimension. Similar findings were reported in previous studies (Dimitrios et al. 2009; Ma et al. 2011).

Effects of nano-ZnO suspensions on germination of Chinese cabbage seeds

Within the range of nano-ZnO concentrations tested (1–80 mg/L), the germination rates of Chinese cabbage seeds were 90–100 % (Fig. 2a) and no significant inhibition was observed compared with the control ( $P > 0.05$ ). However, root and shoot elongation of Chinese cabbage seedlings were significantly inhibited by nano-ZnOs even at low concentrations (1–5 mg/L) ( $P < 0.05$ ) (Fig. 2). As the nano-ZnO concentrations increased, the inhibition of root elongation increased rapidly, but slowly for shoot elongation (Fig. 2b, c). There was a significant negative correlation between the length of roots or shoots and the nano-ZnO concentrations ( $P < 0.05$ ). The  $IC_{50}$  values for root elongation were 37.6, 43.8, 44.1, and 55.3 mg/L for ZnO-30, ZnO-50, ZnO-90, and ZnO-150,

**Fig. 1** SEM or TEM image of four nano-ZnOs. Four nano-ZnOs were determined by TEM or SEM. **a** TEM image of ZnO-30 (~30 nm spheric nanoparticles); **b** TEM image of ZnO-50 (~50 nm spheric nanoparticles); **c** TEM image of ZnO-90 (columniation with bottom surface diameter of 90 nm and height of 400 nm); **d** TEM (1) and SEM (2) images of ZnO-150 (hexagonal rod with hexagon length of 150 nm and height of 600 nm)

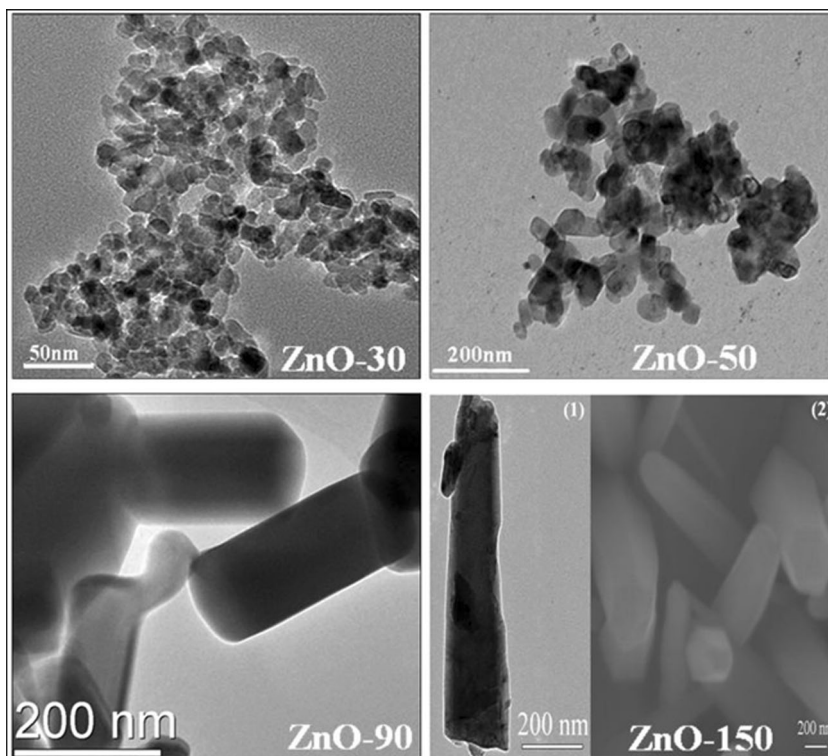
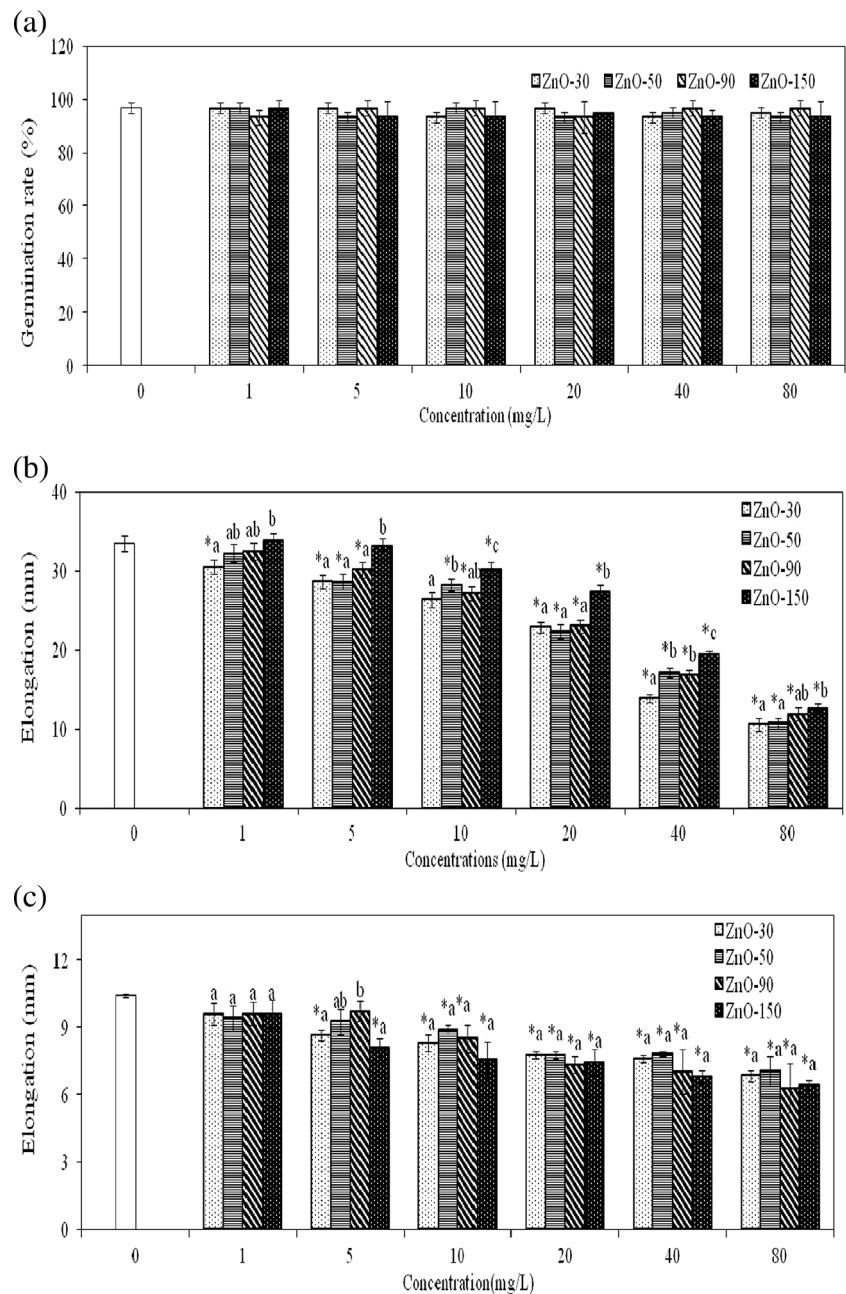


**Fig. 2** Effects of nano-ZnOs on shoot/root elongation of Chinese cabbage seedling. **a** Germination rate, **b** root elongation, **c** shoot elongation. The values are given as means with error bars. The means followed by the same letters within the same nano-ZnO concentration are not statistically different ( $P>0.05$ ). The statistical significance compared nano-ZnO treatments with the control was marked with *asterisk* ( $P<0.05$ )



respectively, which were considerably lower than those of shoot elongation (>80 mg/L; Table 1). More marked inhibitions were found in root elongation than in shoot elongation, indicating that root elongation was more sensitive to nano-ZnO toxicity than shoot elongation.

More interestingly, the nano-ZnOs (ZnO-30) with the smallest primary size caused the greatest inhibition of root elongation, and vice versa (ZnO-150) (Fig. 2b). Additionally, root lengths were subjected to a two-factor variance analysis (Supplementary data Table S1). The results indicated that root lengths could be divided into three significantly different groups, i.e., ZnO-30 (22.14 mm), ZnO-50 (23.18 mm) and ZnO-90 (23.58 mm), and ZnO-150

(26.56 mm), which were positively correlated to the primary size of nano-ZnOs in the minimum dimensionality from 30 to 150 nm. Therefore, the toxicity of nano-ZnOs increased significantly as the size in the minimum dimension decreased. However, the toxicities of the large columnar ZnO-90 and small spherical ZnO-50 were comparable, suggesting that the morphology of nano-ZnOs influenced their toxicity.

Effects of seed soaking in nano-ZnO suspensions on root elongation of Chinese cabbage

The effects of soaking seeds in four nano-ZnO suspensions on root elongation of Chinese cabbage are shown in Fig. S4 of

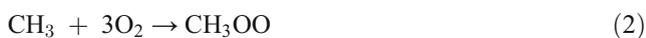
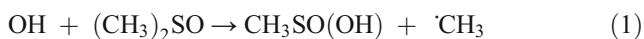
**Table 1** Regression equations between the concentrations of four morphological nano-ZnOs and shoot/root elongation of seedling

Nano-ZnO	Index	Regression equation	R <sup>2</sup>	IC <sub>50</sub> (mg/L)	95 % confidence interval (mg/L)
ZnO-30	Root length	$y=31.67 e^{-0.017x}$	0.967	37.6	(31.9, 44.7)
	Shoot height	$y=9.31 e^{-0.005x}$	0.711	116.1	(89.5, 207.5)
ZnO-50	Root length	$y=32.24 e^{-0.015x}$	0.982	43.8	(37.3, 48.6)
	Shoot height	$y=9.50 e^{-0.004x}$	0.982	150.0	(94.0, 211.8)
ZnO-90	Root length	$y=32.43 e^{-0.0015x}$	0.979	44.2	(39.9, 52.8)
	Shoot height	$y=9.61 e^{-0.007x}$	0.814	87.5	(71.1, 131.0)
ZnO-150	Root length	$y=34.32 e^{-0.013x}$	0.990	55.3	(50.3, 61.2)
	Shoot height	$y=9.031 e^{-0.006x}$	0.629	91.7	(61.0, 202.8)

Supplementary data. Treatment I (ZnO-H<sub>2</sub>O) had no significant effect on root elongation compared with the control (seeds being soaked and incubated in deionized water) ( $P>0.05$ ). However, root elongation was severely inhibited by both treatment II (H<sub>2</sub>O-ZnO) and treatment III (ZnO-ZnO), to a similar degree (Supplementary data Fig. S4). These results indicated that nano-ZnOs could not pass through seed coats, and the toxicity of nano-ZnOs to seed germination occurred mainly during seed incubation rather than seed soaking. This likely explained why seedling growth, but not seed germination rates, was significantly affected by exposure to nano-ZnOs.

Effects of DMSO-treated nano-ZnOs on root elongation of Chinese cabbage

Free hydroxyl groups ( $\cdot$ OH) are important reactive oxygen species (ROS). They can induce oxidative stress, lead to an increase in lipid peroxidation and accumulation of methyl dialdehyde (MDA), which is harmful to normal plant cells (Wang et al. 2011; Xu et al. 2009). Nanoparticles are particularly able to generate cavities, and thus increase the production of ROS (Hao and Chen 2012; Hao et al. 2009). DMSO is a well-known free hydroxyl radical scavenger that can react with and eliminate free hydroxyl groups derived from the surface of nanoparticles. The process is as follows (Yang and Watts 2005; Zhang et al. 2002):



In this study, root elongation was significantly inhibited by both treatment I (1.0 % DMSO) and treatment II (40 mg/L nano-ZnO suspension) compared with the control (deionized water),  $P<0.05$  (Fig. 3). The toxicity of DMSO to root

elongation may be attributed to its high cell permeability and accumulation in Chinese cabbage seedlings (Mittal et al. 2008). However, root elongation of treatment III (40 mg/L nano-ZnOs suspension with 1 % DMSO) was significantly improved by 6–39 % compared with treatments I and II, despite the root lengths being much shorter than the control (Fig. 4). These results indicated that DMSO could significantly reduce the phytotoxicity of nano-ZnOs by scavenging  $\cdot$ OH groups derived from the nano-ZnOs. In order to further prove the occurrence of  $\cdot$ OH groups in nano-ZnO suspensions, isopropyl, which can react with  $\cdot$ OH groups to acetone, was used as a probe to detect free hydroxyl groups ( $\cdot$ OH) derived from nano-ZnOs during germination (Supplementary data Page S2). The results showed that both isopropyl and acetone were found in nano-ZnOs treatments with isopropyl while only isopropyl was observed in isopropyl treatments (Fig. 4), confirming the generation of  $\cdot$ OH groups in nano-ZnO suspensions during germination. Therefore, we speculated that free hydroxyl groups ( $\cdot$ OH) played a key role in the phytotoxicity of nano-ZnOs in terms of inhibition of root elongation of Chinese cabbage seedling.

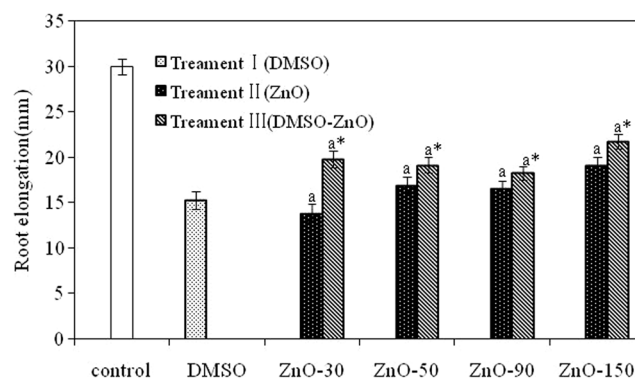
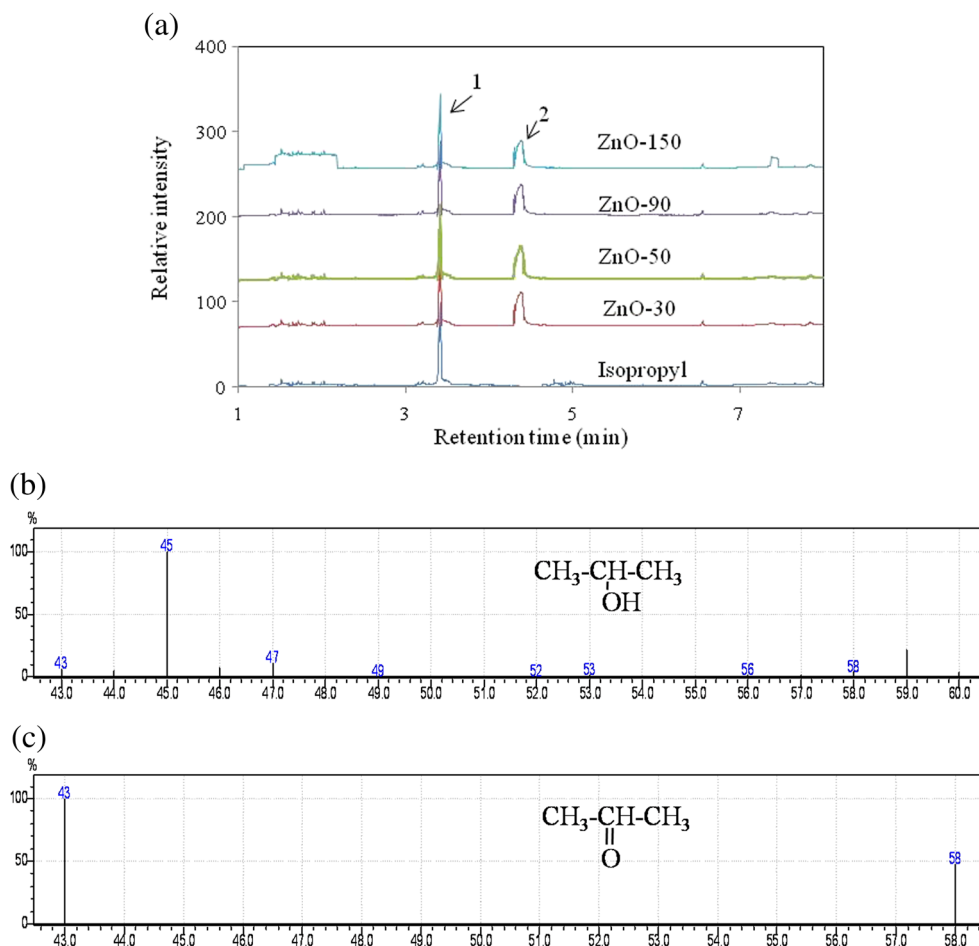


**Fig. 3** Effects of DMSO-treated nano-ZnOs on root elongation of Chinese cabbage seedling. The statistical significance compared treatment II with Treatment III as well as compared treatment groups with the control was marked with “asterisk” and “a,” respectively ( $P<0.05$ )

**Fig. 4** GC-MS chromatograms and mass spectrums of supernatant samples collected from isopropyl treatments and nano-ZnO treatments with isopropyl. **a** Chromatograms; **b** mass spectrums of “1” peak in image **a**; **c** mass spectrums of “2” peak in image **a**. Isopropyl treatments: seeds were grown in a 0.2 % isopropyl (v/v) solution for 72 h. Nano-ZnO (40 mg/L) treatments with isopropyl: seeds were grown in 40 mg/L nano-ZnOs with 0.2 % isopropyl (v/v) for 72 h



Effects of zinc ions in nano-ZnO suspensions on seed germination of Chinese cabbage

The solubility of nanoparticles (especially metal-based nanoparticles) in water is an important factor when assessing their toxicity mechanism (Bai et al. 2010). Concentrations of  $Zn^{2+}$  in nano-ZnO supernatants (after centrifugation and filtration)

before and after 72-h seed germination were measured. The dissolved  $Zn^{2+}$  concentrations (0.2–2.0 mg/L) in the four nano-ZnO supernatants increased with the increase of nano-ZnO concentrations, but the nano-ZnO dissolution rates ( $Zn^{2+}$ /nano-ZnOs) decreased, with the highest dissolved  $Zn^{2+}$  concentrations being less than 5 mg/L (Table 2). At such a low  $Zn^{2+}$  concentration, no significant inhibition of root

**Table 2** Dissolved zinc ions in four morphological nano-ZnO suspensions

Nano-ZnO	Measure time	Concentration (mg/L)						
		1	5	10	20	40	80	
ZnO-30	Before germination	0.37±0.09 Aab	0.97±0.11 Ba	1.11±0.10 BCab	1.26±0.06 CDa	1.43±0.07 DEa	1.48±0.08 Ea	
ZnO-50		0.34±0.05 Aab	0.81±0.12 Ba	0.96±0.14 Ba	1.19±0.05 Ca	1.31±0.09 Ca	1.51±0.16 Da	
ZnO-90		0.50±0.12 Ab	0.95±0.14 Ba	1.12±0.08 BCab	1.18±0.09 BCa	1.16±0.14 CDa	1.37±0.17 Da	
ZnO-150		0.27±0.09 Aa	0.87±0.10 Ba	1.21±0.12 Cb	1.26±0.12 Ca	1.35±0.14 CDa	1.50±0.16 Da	
ZnO-30	After germination	0.51±0.02 Ad	1.65±0.08 Bb	2.04±0.10 Ca	2.91±0.15 Db	3.50±0.17 Eab	4.50±0.33 Fa	
ZnO-50		0.48±0.02 Ac	1.54±0.08 Ba	2.01±0.09 Cb	2.76±0.14 Dab	3.21±0.15 Ea	4.20±0.30 Ea	
ZnO-90		0.42±0.01 Ab	1.62±0.08 Ba	1.95±0.09 Ca	2.80±0.02 Dab	3.72±0.18 Eb	4.32±0.25 Ea	
ZnO-150		0.35±0.01 Aa	1.34±0.02 Ba	1.79±0.08 Ca	2.53±0.13 Da	3.54±0.17 Eb	4.10±0.40 Ea	

For the same measure time, means±SD followed by the same capital letters within the same row or by the small letter within the same column are not statistically different. Statistical significance was accepted at  $P<0.05$

elongation occurred following ZnSO<sub>4</sub> treatments (Supplementary data Fig. S5). Therefore, the dissolved Zn<sup>2+</sup> originating from the nano-ZnOs was not the major reason for the effects of nano-ZnO on Chinese cabbage seedlings.

Uptake of nano-ZnOs by Chinese cabbage seedlings

Total Zn concentrations (including nano-ZnOs and Zn<sup>2+</sup>) in the roots and shoots of Chinese cabbage seedlings following the nano-ZnOs and Zn<sup>2+</sup> treatments were determined. Total Zn concentrations in the tissues of Chinese cabbage seedlings increased with the increase of nano-ZnO and Zn<sup>2+</sup> concentrations. Remarkably, total Zn concentrations in both roots and shoots increased rapidly with decreasing sizes of nano-ZnOs in the minimum dimension (Fig. 5a, b). Moreover, total Zn

concentrations in roots were significantly higher than in shoots for all treatments (Supplementary data Fig. S6), which may partly explain the greater inhibition of root than shoot elongation. The total Zn concentrations of both roots and shoots in the nano-ZnO treatments (1, 10, or 80 mg/L) were significantly higher than in the Zn<sup>2+</sup> treatments (0.5, 2, or 5 mg/L) (Supplementary data Fig. S7), although the Zn<sup>2+</sup> concentrations in nano-ZnO suspensions were lower than or comparable with those Zn<sup>2+</sup> in the form of ZnSO<sub>4</sub> in solutions (Table 2). Therefore, nano-ZnOs might be absorbed directly by Chinese cabbage seedlings. Translocation factors (TFs) of total Zn—defined as the ratio of the total Zn concentration of shoots to roots (Lin and Xing 2008)—were 0.28–0.62, 0.33–0.78, 0.34–1.06, and 0.46–0.88 for ZnO-30, ZnO-50, ZnO-90, and ZnO-150, respectively (Supplementary data Table S2). Generally, TFs in the treatments with larger nano-ZnOs were higher than with smaller nano-ZnOs due to the higher absorption of the latter which were readily fixed into seedling roots but difficultly transported into the shoots. Correlation analysis showed that the degree of inhibition of root and shoot elongation had a significant linear relationship with the total Zn concentrations in roots and shoots, respectively (Table 3). Therefore, the uptake of Zn by Chinese cabbage seedlings was an important source of nano-ZnO phytotoxicity.

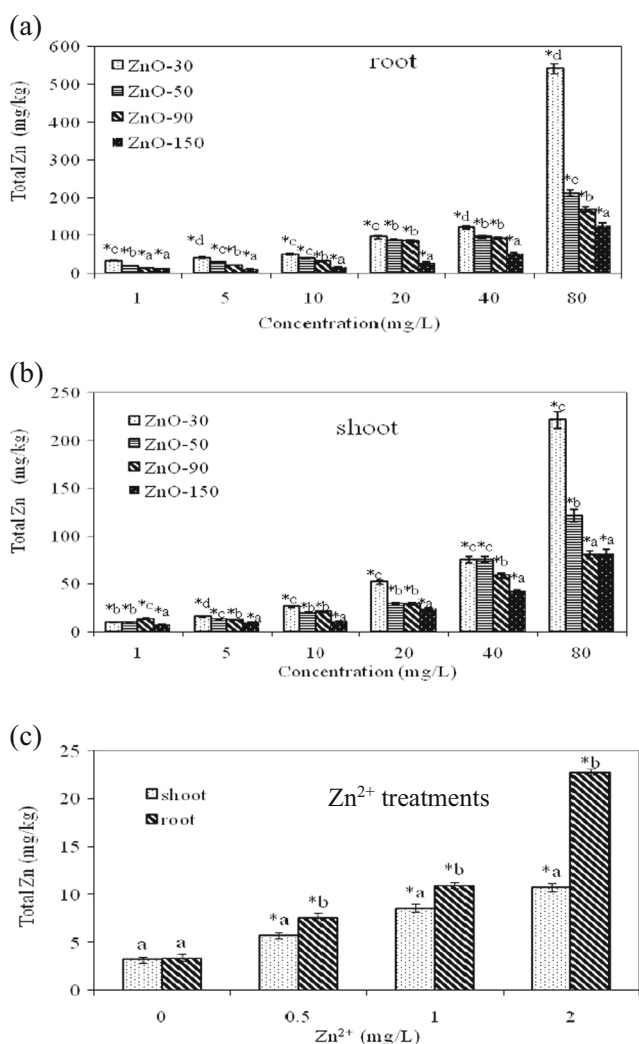


**Fig. 5** The total Zn concentrations in roots and shoots (dry weight) under nano-ZnO treatments and Zn<sup>2+</sup> treatments. The values are given as means with error bars. The means followed by the same letters within the same nano-ZnO concentration are not statistically different ( $P > 0.05$ ). The statistical significance compared nano-ZnO (or Zn<sup>2+</sup>) treatments with the control was marked with asterisk ( $P < 0.05$ )

Discussion

Plant is an important component of ecological systems and may serve as a pathway for nanoparticle transport and as a route for bioaccumulation into the food chain, resulting in negative effects on the environment and human health (Lin and Xing 2007; Ma et al. 2010). Previous studies have shown that the growth of biomass, root length, and shoot height of zucchini (*Cucubita pepo* L.) seedlings were retarded by nanoparticles (including multiwalled carbon nanotubes [MWCNTs], Ag, Cu, and ZnO), but seed germination rates were unaffected (Dimitrios et al. 2009; Service 2003). In this study, similar effects of nanoparticles on seed germination of Chinese cabbage were observed. Both root length and shoot

**Table 3** Linear relationship between inhibitory of root/shoot and total Zn concentrations in roots/shoots

Nano-ZnO	Root		Shoot	
	R <sup>2</sup>	P	R <sup>2</sup>	P
ZnO-30	0.806	0.053	0.833	0.039*
ZnO-50	0.956	0.003*	0.879	0.021*
ZnO-90	0.965	0.002*	0.908	0.012*
ZnO-150	0.940	0.005*	0.770	0.073

The statistical significance was marked with “asterisk” ( $P < 0.05$ )

height were significantly inhibited by the four nano-ZnOs at concentrations of 1–80 mg/L, but there was no significant difference in the seed germination rates of Chinese cabbage between the nano-ZnO treatments and the control. This could be attributed to the seed coats, which have selective permeability and protect the seed from harmful external factors (Lin and Xing 2007; Liu et al. 2009a). Seed soaking in nano-ZnOs followed by incubation in deionized water had no significant effects on root elongation compared with the control. This indicated that nano-ZnOs could not pass through the seed coats, and thus did not inhibit seed germination.

The inhibition of root elongation increased rapidly with increasing nano-ZnO concentrations (1–80 mg/L), but the inhibition of shoot elongation increased slowly. The radicles were in direct contact with the nanoparticles and thus were the first tissue to be exposed to excess concentrations of nano-ZnOs. Therefore, the adverse effects were more marked in roots than in shoots, suggesting that root elongation was more sensitive to nano-ZnO toxicity than shoot elongation (Ma et al. 2010; Xu et al. 2009).

There are various mechanisms of nanotoxicity, in which the chemical composition, surface characteristics (coating, charge, etc.), size, and morphology of nanoparticles play key roles (Xu et al. 2010). In addition to the “dose-effect” relationship, nanotoxicity displays “size-dependent” and “morphology-dependent” tendencies, which is different from traditional pollutants (Chang et al. 2011). Previous studies showed that the toxicity of nano-Zn or nano-Cu to mice increased significantly with the size decrease of the nanoparticles (Liu et al. 2009b; Wang et al. 2006). A similar trend was also observed in this study. The nanoparticle with the smallest primary size (ZnO-30) had the highest phytotoxicity, while the nanoparticle with the largest primary size (ZnO-150) had the lowest phytotoxicity (Table 1, Fig. 2). Treatment with DMSO significantly improved the root elongation of seedlings in 40 mg/L nano-ZnO suspensions, due to its scavenging of free hydroxyl groups ( $\cdot\text{OH}$ ). The enhancement of root elongation in the DMSO-nanoparticle treatments decreased in the order of ZnO-30 (38.8 %)>ZnO-50 (10.5 %)>ZnO-150 (9.8 %)>ZnO-90 (6 %). This indicates that the primary size of nano-ZnOs had a marked effect on their toxicity, which was partly attributed to the difference in  $\cdot\text{OH}$  production of nano-ZnOs, itself derived from surface-catalyzed reactions and stress stimuli induced the size and morphology of the nanoparticles, including cavity formation (Xiong et al. 2011; Yang and Watts 2005).

Generally, smaller particles readily adhere to biological components and generate more notable adverse effects because of their rapidly increasing surface area and energy (Liu et al. 2009b). In this study, the average hydrodynamic diameters of the nano-ZnOs were positively correlated with their sizes in the minimum dimension. Indeed, the surface areas of nano-ZnOs increased markedly as the primary size

decreased in the order spherical ZnO-30 ( $65 \text{ m}^2/\text{g}$ )>spherical ZnO-50 ( $55 \text{ m}^2/\text{g}$ )>columnar ZnO-90 ( $25 \text{ m}^2/\text{g}$ )>hexagon rod-like ZnO-150 ( $12 \text{ m}^2/\text{g}$ ). Thus, the nanoparticle with the smallest primary size (ZnO-30) displayed the greatest toxicity in terms of inhibiting root and shoot elongation, while the nanoparticle with the largest size (ZnO-150) displayed the weakest toxicity; thus, phytotoxicity and primary sizes were significantly negatively correlated (Supplementary data Table S1). However, some studies have reached the controversial conclusion that the sizes of nanoparticles affect their toxicity. A previous study found no significant difference in toxicity to zebrafish (*Danio rerio*) for nano-Ni spheres of sizes 30–100 nm (Ispas et al. 2009). Another study found that the cytotoxicity of 24 nanomaterials (nano-TiO<sub>2</sub>, nano-Ag, and nano-Co) to human pulmonary cells did not depend on their sizes (Lanone et al. 2009). These discrepancies may be related to the variation in nanoparticle concentrations and size range and the biological target tested. Chang et al. (2011) reported a size threshold for size-dependent nanotoxicity. At sizes under this threshold, nanoparticles exerted marked adverse effects on biological targets; furthermore, nanotoxicity increased rapidly with decreasing size. However, no such effect was observed when the primary sizes of nanoparticles exceeded the size thresholds (Chang et al. 2011).

The morphology of nanoparticles also plays a key role in their toxicity. One study reported a significant difference in toxicity to macrophages between two carbon nanotubes with distinct morphologies (MWCNTs and SWCNTs) (Jia et al. 2005). In this study, the phytotoxicity of the small ZnO-50 spheres and the large ZnO-90 columns was comparable (Fig. 2, Table 1), which does not support the concept of size-dependent toxicity, instead suggesting a morphology-dependent tendency. The differences in the morphology of nanoparticles may alter the sites and strength of the interaction between the particles and their biological targets, leading to a difference in toxicity (Chang et al. 2011). Some properties (e.g., solubility, ROS productivity) of nanoparticles change markedly when their morphology changes (Clement et al. 2013). In this study, the root and shoot concentrations of Zn<sup>2+</sup> and total Zn, as well as ROS productivity, of the ZnO-50 treatment were comparable to those of the ZnO-90 treatment (Table 2, Figs. 3, 4, and 5). This indicates that differences in morphology influenced the size-dependent toxicity of nanoparticles, leading to comparable toxicity between large column (ZnO-90) and small sphere (ZnO-50) nanoparticles.

Zinc is an essential element for plants, animals, and humans. However, various biological targets can be damaged by high zinc levels (Wang et al. 2006). A previous study showed that the toxicity of nano-ZnO to microalga was attributed to the release of zinc ions (Franklin et al. 2007). Another study showed that exposure to a nano-ZnO suspension significantly reduced maize root elongation, but zinc ions dissolving from nano-ZnOs had no effect on root growth (Lin and Xing

2007). These discrepancies in findings are likely related to various complicating factors, including differences in nanoparticle solubility and the sensitivity of the biological targets tested. In this study, the  $Zn^{2+}$  concentrations in nano-ZnO suspensions were less than 5 mg/L, which had no effect on the root and shoot elongation of Chinese cabbage. However, the total Zn concentrations in the roots and shoots were considerably higher for nano-ZnO than  $Zn^{2+}$  treatments. A significant linear relationship was observed between the Zn concentrations in roots or shoots and the degree of inhibition of root or shoot elongation for the nano-ZnO treatments (Table 3). This indicated that nano-ZnOs might be absorbed and transported by Chinese cabbage seedlings, leading to an adverse effect on roots and shoots in vivo. Our results are consistent with a previous report that nano-ZnOs were readily adhered to the root surface of ryegrass and were taken up in vivo (Lin and Xing 2008), but the TFs of total Zn in ryegrass (0.01–0.02) for ZnO nanoparticle treatments were considerably lower than those reported in this study. This difference may be attributable to the variation of experimental conditions and nano-ZnO translocation rates among different plant species. In our study, Chinese cabbage seeds were incubated in sealed petri dishes containing nano-ZnO suspensions for only 72 h. In such a short time, the Casparian strip, which determines the interchange of materials between roots and shoots, did not form completely; thus, Chinese cabbage seedlings were prone to take up and transport nano-ZnOs into shoots during germination (Peterson and Lefcounrt 1990). In a previous study (Lin and Xing 2008), ryegrass seedlings were grown in nano-ZnO suspensions containing elemental nutrients for 2 weeks, allowing the Casparian strip between the roots and shoots of ryegrass seedlings to form completely, and thus prevent transport of nano-ZnOs into the shoot. Therefore, the total Zn concentrations in shoots and their TFs were higher in the nano-ZnO treatments in this study.

In addition, the pH values of the supernatants of the nano-ZnO suspensions ranged from 6.7 to 7.3 (Supplementary data Table S3) before and after the seed germination experiments, which has been reported to have no adverse effect on seed germination of plant (Lin and Xing 2007).

## Conclusions

Within the concentration range investigated (1–80 mg/L), four nano-ZnOs had no obvious effects on the seed germination rates of Chinese cabbage but significantly inhibited the root and shoot elongation of seedlings. Both the primary size in the minimum dimension and the morphology of nano-ZnOs affected their toxicity. Generally, the smaller nano-ZnOs displayed the greater toxicity. Both the production of ·OH groups and the bioaccumulation of nano-ZnOs played key

roles in their toxicity, while the  $Zn^{2+}$  released from nano-ZnOs had a negligible toxic effect.

**Acknowledgments** This work was financially supported by the National Natural Science Foundation of China (41071211, 41173101, and 41301337).

## References

- Bai W, Zhang ZY, Tian WJ, He X, Ma YH, Zhao YL, Chai ZF (2010) Toxicity of zinc oxide nanoparticles to zebrafish embryo: a physicochemical study of toxicity mechanism. *J Nanopart Res* 12:1645–1654. doi:10.1007/s11051-009-9740-9
- Chang X, Zu Y, Zhao Y (2011) Size and structure effects in the nanotoxic response of nanomaterials. *Chin Sci Bull* 56:108–118. doi:10.1360/972010-1640
- Clement L, Hurel C, Marmier N (2013) Toxicity of TiO<sub>2</sub> nanoparticles to cladocerans, algae, rotifers and plants - Effects of size and crystalline structure. *Chemosphere* 90:1083–1090. doi:10.1016/j.chemosphere.2012.09.013
- Dietz K-J, Herth S (2011) Plant nanotoxicology. *Trends Plant Sci* 16:582–589. doi:10.1016/j.tplants.2011.08.003
- Dimitrios S, Saion KS, Jason CW (2009) Assay-dependent phytotoxicity of nanoparticles to plants. *Environ Sci Technol* 43:9473–9479. doi:10.1007/s11051-013-1829-5
- Franklin NM, Rogers NJ, Apte SC, Batley GE, Gadd GE, Casey PS (2007) Comparative toxicity of nanoparticulate ZnO, bulk ZnO, and ZnCl<sub>2</sub> to a freshwater microalga (*Pseudokirchneriella subcapitata*): the importance of particle solubility. *Environ Sci Technol* 41:8484–8490. doi:10.1021/es071445r
- Ghodake G, Seo YD, Lee DS (2011) Hazardous phytotoxic nature of cobalt and zinc oxide nanoparticles assessed using *Allium cepa*. *J Hazard Mater* 186:952–955. doi:10.1016/j.jhazmat.2010.11.018
- Gottschalk F, Sonderer T, Scholz RW, Nowack B (2009) Modeled environmental concentrations of engineered nanomaterials (TiO<sub>2</sub>, ZnO, Ag, CNT, Fullerenes) for different regions. *Environ Sci Technol* 43:9216–9222. doi:10.1021/es9015553
- Hao LH, Chen L (2012) Oxidative stress responses in different organs of carp (*Cyprinus carpio*) with exposure to ZnO nanoparticles. *Ecotox Environ Safe* 80:103–110. doi:10.1016/j.ecoenv.2012.02.017
- Hao LH, Wang ZY, Xing BS (2009) Effect of sub-acute exposure to TiO<sub>2</sub> nanoparticles on oxidative stress and histopathological changes in Juvenile Carp (*Cyprinus carpio*). *J Environ Sci-China* 21:1459–1466. doi:10.1016/s1001-0742(08)62440-7
- Hu XG, Zhou QX (2014) Novel hydrated graphene ribbon unexpectedly promotes aged seed germination and root differentiation. *Sci Rep* 4:3782
- Ispas C, Andreescu D, Patel A, Goia DV, Andreescu S, Wallace KN (2009) Toxicity and developmental defects of different sizes and shape nickel nanoparticles in zebrafish. *Environ Sci Technol* 43:6349–6356. doi:10.1021/es9010543
- Jia G, Wang HF, Yan L, Wang X, Pei RJ, Yan T, Zhao YJ, Guo XB (2005) Cytotoxicity of carbon nanomaterials: single-wall nanotube, multi-wall nanotube, and fullerene. *Environ Sci Technol* 39:1378–1383. doi:10.1021/es0487291
- Judy JD, Urline JM, Bertsch PM (2011) Evidence for biomagnification of gold nanoparticles within a terrestrial food chain. *Environ Sci Technol* 45:776–781. doi:10.1021/es103031a
- Kaegi R, Voegelin A, Simmet B, Zuleeg S, Hagedorfer H, Burkhardt M, Siegrist H (2011) Behavior of metallic silver nanoparticles in a pilot wastewater treatment plant. *Environ Sci Technol* 45:3902–3908. doi:10.1021/es1041892

- Kool PL, Ortiz MD, van Geste CAM (2011) Chronic toxicity of ZnO nanoparticles, non-nano ZnO and ZnCl<sub>2</sub> to *folsomia candida* (*Collembola*) in relation to bioavailability in soil. *Environ Pollut* 159:2713–2719. doi:10.1016/j.envpol.2011.05.021
- Kordon H (1992) Seed viability and germination: a multi-purpose experimental system. *J Biol Educ* 26:247–251. doi:10.1080/00219266.1992.9655281
- Lanone S, Rogerieux F, Geys J, Dupont A, Maillot-Marechal E, Boczkowski J, Lacroix G, Hoet P (2009) Comparative toxicity of 24 manufactured nanoparticles in human alveolar epithelial and macrophage cell lines. *Part Fibre Toxicol* 6:1–12. doi:10.1186/1743-8977-6-14
- Lin D, Xing B (2007) Phytotoxicity of nanoparticles: inhibition of seed germination and root growth. *Environ Pollut* 150:243–250. doi:10.1016/j.envpol.2007.01.016
- Lin DH, Xing BS (2008) Root uptake and phytotoxicity of ZnO nanoparticles. *Environ Sci Technol* 42:5580–5585. doi:10.1021/es800422x
- Liu TF, Wang T, Sun C, Wang YM (2009a) Single and joint toxicity of cypermethrin and copper on Chinese cabbage (Pakchoi) seeds. *J Hazard Mater* 163:344–348. doi:10.1016/j.jhazmat.2008.06.099
- Liu Y, Gao Y, Zhang L, Wang T, Wang J, Jiao F, Li W, Liu Y, Li YF, Li B, Chai ZF, Wu G, Chen CY (2009b) Potential health impact on mice after nasal instillation of nano-sized copper particles and their translocation in mice. *J Nanosci Nanotechnol* 9:6335–6343. doi:10.1166/jnn.2009.1320
- Luna-delRisco M, Orupold K, Dubourguier HC (2011) Particle-size effect of CuO and ZnO on biogas and methane production during anaerobic digestion. *J Hazard Mater* 189:603–608. doi:10.1016/j.jhazmat.2011.02.085
- Ma YH, Kuang LL, He X, Bai W, Ding YY, Zhang ZY, Zhao YL, Chai ZF (2010) Effects of rare earth oxide nanoparticles on root elongation of plants. *Chemosphere* 78:273–279. doi:10.1016/j.chemosphere.2009.10.050
- Ma H, Kabengi NJ, Bertsch PM, Unrine JM, Unrine JM, Glenn TC, Williams PL (2011) Comparative phototoxicity of nanoparticulate and bulk ZnO to a free-living nematode *Canorhabditis elegans*: the importance of illumination mode and primary particle size. *Environ Pollut* 159:1473–1480. doi:10.1016/j.envpol.2011.03.013
- Mittal A, Sara UVS, Ali A, Aqil M (2008) The effect of penetration enhancers on permeation kinetics of nitrendipine in two different skin models. *Biol Pharm Bull* 31:1766–1772. doi:10.1248/bpb.31.1766
- Nair R, Varghese SH, Nair BG, Maekawa T, Yoshida Y, Kumar DS (2010) Nanoparticulate material delivery to plants. *Plant Sci* 179:154–163. doi:10.1016/j.plantsci.2010.04.012
- Peterson CA, Lefcounrt BEM (1990) Development of endodermal casparian bands and xylem in lateral roots of broad bean. *Can J Bot* 68:2729–2735. doi:10.1016/j.envpol.2013.11.014
- Poynton HC, Lazorchak JM, Impellitteri CA, Smith ME, Rogers K, Patra M, Hammer KA, Allen HJ, Vulpe CD (2011) Differential gene expression in daphnia magna suggests distinct modes of action and bioavailability for ZnO nanoparticles and Zn ions. *Environ Sci Technol* 45:762–768. doi:10.1021/es102501z
- Rico CM, Majumdar S, Duarte-Gardea M, Peralta-Videa JR, Gardea-Torresdey JL (2011) Interaction of nanoparticles with edible plants and their possible implications in the food chain. *J Agr Food Chem* 59:3485–3498. doi:10.1021/jf104517j
- Rousk J, Ackermann K, Curling SF, Jones DL (2012) Comparative toxicity of nanoparticulate CuO and ZnO to soil bacterial communities. *PLoS One* 7:34197–34197. doi:10.1371/journal.pone.0034197
- Wang B, Feng WY, Wang TC, Guang J, Wang M, Shi JW, Zhang F, Zhao YL, Chai ZF (2006) Acute toxicity of nano- and micro-scale zinc powder in healthy adult mice. *Toxicol Lett* 161:115–123. doi:10.1016/j.toxlet.2005.08.007
- Wang Z, Xiao BD, Song LR, Wu XQ, Zhang JQ, Wang CB (2011) Effects of microcystin-LR, linear alkylbenzene sulfonate and their mixture on lettuce (*Lactuca sativa* L.) seeds and seedlings. *Ecotoxicology* 20:803–814. doi:10.1016/j.toxlet.2005.08.007
- Wang ZY, Xie XY, Zhao J, Liu XY, Feng WQ, White JC, Xing BS (2012) Xylem- and phloem-based transport of CuO nanoparticles in maize (*Zea mays* L.). *Environ Sci Technol* 46:4434–4441. doi:10.1021/es204212z
- Xiong D, Fang T, Yu L, Sima X, Zhu W (2011) Effects of nano-scale TiO<sub>2</sub>, ZnO and their bulk counterparts on zebrafish: acute toxicity, oxidative stress and oxidative damage. *Sci Total Environ* 409:1444–1452. doi:10.1016/j.scitotenv.2011.01.015
- Xu ZQ, Zhou QX, Liu WT (2009) Joint effects of cadmium and lead on seedlings of four Chinese cabbage cultivars in northeastern China. *J Environ Sci-China* 21:1598–1606. doi:10.1016/s1001-0742(08)62461-4
- Xu M, Fujita D, Kajiwara S, Minowa T, Li X, Takemura T, Iwai H, Hanagata N (2010) Contribution of physicochemical characteristics of nano-oxides to cytotoxicity. *Biomaterials* 31:8022–8031. doi:10.1016/j.biomaterials.2010.06.022
- Yang L, Watts DJ (2005) Particle surface characteristics may play an important role in phytotoxicity of alumina nanoparticles. *Toxicol Lett* 158:122–132. doi:10.1016/j.toxlet.2005.03.003
- Zhai T, Xie SL, Zhao YF, Sun XF, Lu XH, Yu MH, Xu FM, Tong YX (2012) Controllable synthesis of hierarchical ZnO nanodisks for highly photocatalytic activity. *Crystengcomm* 14:1850–1855. doi:10.1039/c1ce06013a
- Zhang WX, Karn B (2005) Nanoscale environmental science and technology: challenges and opportunities. *Environ Sci Technol* 39:94A–95A. doi:10.1021/es053197+
- Zhang L, Somasundaran P, Mielczarski J, Mielczarski E (2002) Adsorption mechanism of n-dodecyl-β-D-maltoside on alumina. *J Colloid Interface Sci* 256:16–22. doi:10.1006/jcis.2001.7858
- Zhang Y, Chen Y, Westerhoff P, Hristovski K, Crittenden JC (2008) Stability of commercial metal oxide nanoparticles in water. *Water Res* 42:2204–2212. doi:10.1016/j.watres.2007.11.036
- Zhang P, Ma YH, Zhang ZY, He X, Guo Z, Tai RZ, Ding YY, Zhao YL, Chai ZF (2012) Comparative toxicity of nanoparticulate/bulk Yb<sub>2</sub>O<sub>3</sub> and YbCl<sub>3</sub> to cucumber (*Cucumis sativus*). *Environ Sci Technol* 46:1834–1841. doi:10.1021/es2027295
- Zhu H, Han J, Xiao JQ, Jin Y (2008) Uptake, translocation, and accumulation of manufactured iron oxide nanoparticles by pumpkin plants. *J Environ Monit* 10:713–717. doi:10.1039/b805998e